HIGH-FIDELITY MULTI-PHYSICS COUPLING FOR PREDICTION OF ANISOTROPIC POWER AND TEMPERATURE DISTRIBUTIONSIN FUEL ROD: IMPACT ON HYDRIDE DISTRIBUTION

I. J.Davis[1], O. F.Courty[1], M. N.Avramova[1], A.T. Motta[1] and K. N.Ivanov[1]
[1]Department of Mechanical and Nuclear Engineering,
Penn State University, University Park, PA, USA

ijd5004@psu.edu, o.courty@gmail.com, mna109@psu.edu, atm2@psu.edu, kni1@psu.edu

ABSTRACT

Hydrogen absorbed into the nuclear fuel cladding during reactor exposure is distributed in highly inhomogeneous fashion as a result of temperature and stress gradients. To correctly describe and predict this hydrogen distribution there exists a need for multi-physics coupling to provide accurate azimuthal, radial, and axial temperature distributions in the cladding. This project was created with the idea of providing accurate thermal-hydraulic models for heat transfer by coupling a sub-channel code to a neutronics code and a fuel performance code. The thermal-hydraulics code version chosen is COBRA-TF (CTF), which is a sub-channel code that was modernized and further developed at Penn State University (PSU). CTF's capabilities include modeling two-phase flow in transient or quasi-steady state conditions for light water reactor design and safety analysis. The neutronics code used in this research is DeCART (supported the University of Michigan (UM)), a code which uses the method of characteristics approach to calculate the 3-D neutron flux. For this project, a 4x4 array of fuel rods containing UO_2 fuel surrounded by Zircaloy cladding from a PWR assembly and developed with DeCART were modeled in CTF. The fuel rods selected are from the hottest assembly in the core, which correlates to the highest risk area in the reactor. The power distribution with respect to (x,y,z) coordinates calculated with DeCART was used to calculate the radial power fraction (ratio of power produced in one fuel pin to the power averaged over all the fuel pins in the array), and the axial and radial pin power distributions for input in CTF. This data was, in turn, used to generate the temperature and stress distributions in the cladding. To do this, CTF was coupled to the fuel performance code BISON. BISON is a finite element code developed by Idaho National Laboratory (INL) to study all aspects of thermal and mechanical behavior of fuel rods in the reactor core. Bulk coolant temperature distributions from CTF and power distributions from DeCART are used to accurately model single fuel pins in BISON, which will calculate temperature gradients in the cladding material. Results of these multi-physics calculations are be presented and analyzed in this paper.

1. INTRODUCTION

1.1 Project Goals

The overall purpose of this project is to create accurate and useful means for predicting the distribution of hydrogen in nuclear fuel cladding. To accomplish this overarching goal, several tasks must be performed. First, an analytical model needs to be developed to allow the hydrogen distribution to be calculated from other physical parameters that can be measured or calculated. It is well known that the distribution of hydrogen in cladding is heavily dependent on the temperature and temperature gradient, as explained in more detail in the next section. Thus, tools are needed to model the temperature distribution accurately and efficiently. For the scope of this project, CTF, DeCART, and BISON were chosen. Combing the strengths of each code allows for a more realistic prediction of the temperature gradients inside the cladding during operation. Using accurate temperature maps for the cladding, the analytical model can be used to determine areas of significant hydrogen concentration inside the cladding. In the final analysis, a better understanding of how and where hydrogen distributes in the cladding can help the nuclear industry to predict and prevent future potential fuel failures.

1.2 Background Information

1.2.1 Importance of Hydrogen Study in LWR

The core of a Light-Water Reactor (LWR) contains fuel assemblies cooled by water. A fuel assembly consists of an assemblage of fuel rods (approximately 4 m in height and 9.6 mm in diameter) that contain fissile material in the form of uranium dioxide pellets (UO_2). These fuel rods are sheathed in nuclear fuel cladding, which is made of zirconium alloy and which serves as the primary barrier to contain fission products.

Zirconium alloys have been chosen as cladding material primarily for their very low thermal neutron absorption cross section (0.185 barns (or $0.185 \times 10^{-24} cm^2$) for 0.0253eV neutrons), which allows for good neutron economy [1]. Zirconium alloys also exhibit good corrosion resistance, good heat transfer properties, and appropriate mechanical strength for reactor conditions. Although radiation damage changes cladding properties, these changes tend to saturate after a short reactor exposure and further degradation can occur by corrosion and hydriding[2].

During in-reactor operation, the zirconium cladding is subject to environmental degradation. The cladding tube is under stress from the pressure of the fission gases emitted from the uranium pellet and at high burnup can eventually chemically bond with the pellet itself. Also, the cladding tube is water cooled at its external boundary, which leads to corrosion. The corrosion reaction generates hydrogen, a fraction of which is absorbed by the cladding[3]. Due to the heating of the fuel at its internal boundary, the cladding is submitted to a radial temperature gradient. It is also submitted to an axial gradient, due to the axial heating of the coolant. Geometric heterogeneity (guide tube, corner of assembly, etc.) can lead to azimuthal temperature variations as well. These temperature gradients create a specific distribution of the hydrides in the cladding, as explained in the next sections. Additional sources of hydrogen are water radiolysis and hydrogen added to the reactor core primary water.

The hydrogen picked up by the cladding precipitates at low temperature, which can embrittle the cladding and compromise cladding integrity. An accurate estimation of the amount of precipitated hydrogen allows the identification of the areas more at risk for developing cracks and failures.

1.2.2 Hydrogen Production and Pick-up

As discussed in Section 1.1, in the reactor environment hydrogen can enter the zirconium cladding. The hydrogen entering the cladding originates from several sources. The main source is the waterside corrosion reaction shown below, which generates hydrogen that can be absorbed by the cladding:

$$Zr + 2H_20 \rightarrow ZrO_2 + 4H \quad (1)$$

Some of the hydrogen atoms mentioned above are transported to the oxide-metal interface and can be absorbed into the cladding, a process called hydrogen pick-up. The absorbed hydrogen migrates through the material in response to the thermodynamic driving forces, of concentration, stress and thermal gradients. For Zircaloy-4, 10-20% of the hydrogen liberated from corrosion is typically absorbed into the cladding. Many factors influence hydrogen pick-up, such as oxide film characteristics, alloy composition, temperature residual stresses, area exposed to corrosion and water chemistry.

1.2.3 Hydrogen Redistribution in the Cladding

The hydrogen picked up at the cladding external boundary redistributes via solid state diffusion and precipitates as hydrides (mainly δ-hydrides). Specific hydride distributions form, with a high concentration rim close to the external boundary and a very small one close to the internal boundary, as exemplified below[4].

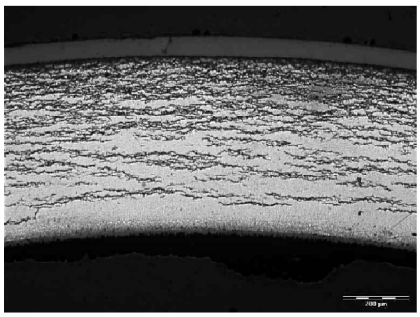

Figure 1 – Optical micrograph of the hydride distribution and oxide layers on Zircaloy-4 irradiated for 6 cycles in a PWR [4].

The hydride distribution resulting from the imposition of a temperature gradient can be modeled if thethree phenomena of Fick's diffusion, Soret effect and precipitation are appropriately taken into account.

1.2.4 Diffusion mechanisms

Two hydrogen solid state diffusion mechanisms can occur in the cladding: diffusion driven by concentration gradient (Fick's law) and diffusion caused by a temperature gradient (Soret effect). Assuming linear thermodynamics, the diffusion flux of dissolved hydrogen in the Zr matrix is given by [5]:

$$J = -\frac{DN}{RT}\left(RT \times \frac{d(\ln(N))}{dx} + \frac{Q^*}{T} \times \frac{dT}{dx} \right) \quad (2)$$

Where **J** is the diffusion flux, D is the diffusion coefficient of H in Zr, **N** is the concentration of hydrogen in solid solution, **R** is the gas constant, **T** is the temperature, and **Q*** is the heat of transport (according to the Soret effect).

1.2.5 Hydride Precipitation

The precipitation of hydrogen in Zirconium is governed by the Terminal Solid Solubility (TSS). This TSS follows an Arrhenius law and is different for hydride precipitation and dissolution[6, 7]. This difference creates a hysteresis effect, such that the precipitation temperature is lower than the dissolution temperature. In this study we do not explicitly model hydride precipitation.

1.2.6 Precipitation kinetics and hydrogen balance

To represent the kinetics of hydrogen migration, the linear model proposed by Marino is used [8, 9]. It leads to the following balance equation:

$$\frac{dC}{dt} = -\nabla J - \alpha^2 (C - C_{eq}) \tag{3}$$

Where, **J** is the diffusion flux (including Fick's law and Soret effect), **α** is the precipitation rate, as defined in [9], **C** is the concentration of hydrogen in solid solution, and $\mathbf{C_{eq}}$ is the equilibrium concentration given by the precipitation Terminal Solid Solubility [7]

1.2.7 Necessity of an accurate temperature prediction

Equations 2 and 3 imply a strong dependence of hydrogen distribution on temperature.[10]. For these reasons, an accurate prediction of the temperature, based on the coupling of Thermal-Hydraulics (T-H), neutronics and fuel performance codes is necessary.

2. DESCRIPTION OF CODES

2.1 CTF

CTF (COBRA-TF) is a two-fluid, three-field subchannel analysis code capable of modeling any vertical one-, two-, or three-dimensional component in the reactor vessel. CTF is an improved version of COBRA-TF that was developed at Penn State University[11].In CTF the fluid field is divided into a continuous liquid field, an entrained liquid drop field, and a vapor field. Like many thermal-hydraulic analysis codes, the equations of the flow field in CTF are solved using a staggered difference scheme in which the velocities are obtained at the mesh faces and the state variables are obtained at the cell center. CTF allows heat transfer surfaces and solid structures that interact significantly with the fluid to be modeled as rods and unheated conductors. CTF allows many parameters to be specified by the user or determined using benchmarked empirical correlations. In the last decade, CTF has been improved (including translation to FORTRAN 95), further developed and extensively validated for both PWR and BWR applications. Attention has been given to improving code error checking and the input deck has been converted from fixed to free format. Then Krylov solver based numerical techniques have been implemented to enhance computational efficiency. Improvements have been made to the turbulent mixing and direct heating models and code quality assurance testing has been performed using an extensive validation and verification matrix. Finally, to improve code usability and enable easier future modifications and improvements, code documentation (including theory, programming, and user manuals) have been prepared. Nowadays it is one of the state-of-the-art codes for LWR thermal-hydraulic analyses.

2.2 DeCART

DeCART (Deterministic Core Analysis based on Ray Tracing) is a method of characteristics neutronics code [12, 13]. DeCART was originally developed by KAERI as part of a US-ROK collaborative I-NERI project between KAERI, ANL, and Purdue University.DOE, EPRI, and AFCI have supported further development in the U.S.T he University of Michigan is also a major supporter of DeCART and its development. Regarding the actual models in the code, DeCART is capable of modeling whole core simulations while calculating direct sub-pin level heterogeneous fluxes at power generating conditions of a PWR and BWR. Also, depletion and transient simulations are available. Input parameters include geometry, material composition, thermal operating conditions, and program execution control parameters.

2.3 BISON

BISON is a nuclear fuel performance analysis tool that is currently under development at the Idaho National Laboratory in the United States[14, 15]. BISON was built using MOOSE (Multiphsics Object Oriented Simulation Environment)[16]. Basically, MOOSE is a multi-physics application framework designed to significantly reduce the expense and time required to develop new applications. BISON is a finite element code that can model a single fuel pin, individual fuel pellet(s), or any single geometry element desired in two or three dimensions. Input parameters include the mesh file for geometry, operating conditions, thermal and mechanical boundary conditions, etc. BISON stores all output information to the mesh file, which can be analyzed in a visualization tool, such as Paraview.

3. DESCRIPTION OF CODE COUPLING

For the purpose of this project, CTF was externally coupled (offline) to both DeCART and BISON.

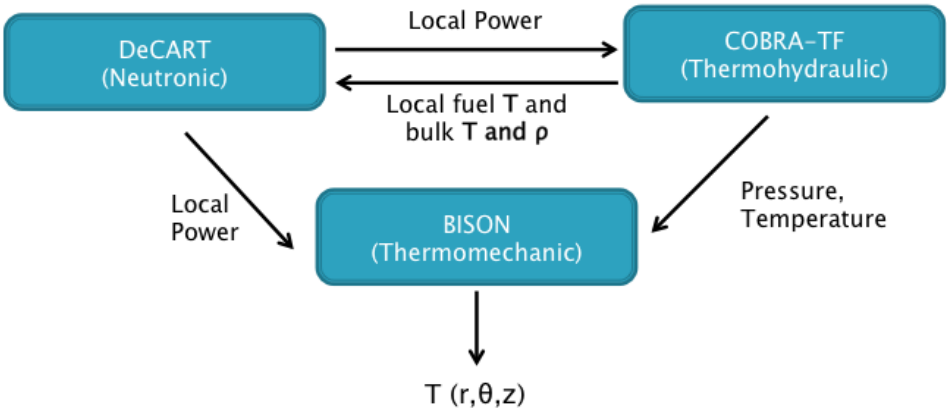

Figure 2 – External coupling diagram between CTF, DeCART, and BISON.

3.1 CTF to DeCART Coupling

In the axial direction (z), the spatial coupling between DeCART and CTF is one-to-one[11, 12]. It should be noted that DeCART can model the areas of the fuel rod below and above the active fuel rod (i.e. the plenum). CTF does not model this region; CTF models from the bottom of the fuel rod to the top. In the radial direction (r), the spatial coupling between DeCART and CTF is one-to-one. The number of radial nodes used in DeCART and CTF can vary based on user

preference. However, CTF only needs radial node input for the fuel region because this is the only heat producing region. Radial nodes may be added to the cladding, but they are not necessary for input data needed from DeCART.This should be kept in mind when including radial nodes in the DeCART input files. The spatial coupling in the azimuthal direction (θ) can vary between DeCART and CTF. DeCART has a number of options for azimuthal splicing of the cells. The choice of azimuthal dependence affects how the output is presented in DeCART. It should be noted that the CTF input cards do not have azimuthal dependence. The azimuthal dependence of fluid temperature comes from the selection of sub-channels surrounding the fuel rod. Therefore, if the DeCART model is split up into 4 or 8 azimuthal regions, data manipulation will need to be performed in order to be transferred correctly in the CTF input cards.

Based on fuel specifications and all known general parameters, input files are made for both DeCART and CTF. At the beginning of calculations, the fuel, clad, and moderator temperatures and densities are be input as nominal values in the DeCART input file. First, DeCART is run. DeCART automatically makes a separate output file for the 3D power distribution at each axial node and burnup step. These output files are manipulated into a form that CTF can understand. CTF can input radial power factors (ratio of the power in one rod to the average power of the array), the radial power distribution for each rod, and the axial power distribution for each rod. Each spliced 3D cell has some associated volume with it. This associated volume is used to weight the volumetric power in each cell to be able to calculate the normalized power distribution for CTF.

Once the radial power factors and power distributions are calculated, CTF is run. Relevant results from CTF output include bulk coolant temperature and density, cladding inner and outer surface temperatures, fuel pellet surface temperature, and fuel pellet centerline temperature. These results are given with respect to the axial direction, and also split into four azimuthal regions. Since the CTF results are given in separate azimuthal sections, data manipulation is performed to be input into DeCART. Refer to Figure 3 to see how subchannels between fuel rods are split up.

3.2 CTF to BISON

Since BISON is a finite element code, the coupling between it and CTF cannot be one-to-one. BISON requires a separate mesh file, which is significantly finer than any CTF input[11, 15]. However, BISON does not require boundary conditions to be placed on every single node. Boundary conditions can be taken with respect to the axial and radial directions in meters. Therefore, the coupling from CTF to BISON is pseudo-one-to-one.A lso, BISON can only model one fuel pin at a time. Therefore, a 4x4 array of fuel pins modeled in a single CTF input will need 16 BISON input files to run. Current plans are to pick the “hottest” pin found in the CTF and DeCART calculations to be modeled in BISON. Because BISON is using finite element method, the code is very computationally expensive and modeling 16 two- or three-dimensional pins separately in BISON is not practical. Based on the fuel specifications and all known general parameters, input files are made for both CTF and BISON. Previous iterations between CTF and DeCART shall be carried out before this step. Results from CTF needed for BISON calculations include the outer surface temperature of the cladding. This temperature distribution is used as a boundary condition in BISON. Based on the BISON model, the cladding temperatures can be input as steady state or time dependent. Also, spatial dependence in the axial and azimuthal directions depends on the BISON model that is created (i.e. 2D or 3D).

3.3 DeCART to BISON

Similar to CTF and BISON, the spatial coupling between DeCART and BISON is not one-to-one. However, the input structure of BISON allows for flexibility when including neutronics data. It can be assumed that working input files have been generated for both DeCART and BISON. Similar to the way DeCART power data was manipulated for CTF, BISON utilizes normalized axial peaking factors for its single pin model[15]. It is important to note that the ability to add radial and azimuthal dependence on peaking factors exists. To explain how to do this, one must first understand how the peaking factors are applied in BISON. Generally, the axial peaking factors are supplied to BISON with a power history in W/m. The local power associated with some axial location of the fuel rod can be calculated by multiplying the linear heat rate in W/m (from the power history) with the axial peaking factor at that location. Thus, the power shape of the fuel rod in the axial direction is known. BISON then calculates the radial peaking factors by itself to map out the rest of the power distribution in the fuel. An alternative way to represent the power distribution in BISON is to supply the fission rates. A fission rate distribution would be able to be calculated from the power distribution from DeCART, along with the energy per fission.

4. RESULTS

For this project, a 4x4 pin array was modeled in CTF and DeCART. This array was modeled after a typical PWR, and all important specifications can be seen in Table 1.Some specifications were taken from a study done at Oak Ridge National Laboratory (ORNL), using the Advanced Multi-Physics Nuclear Fuel Performance Code (AMPFuel) [17]. Other specifications were taken from typical PWR inputs built for use in SIMULATE-3, as part of the university version of the Studsvik Scandpower Code System (CMS) for research and education purposes[18].Using DeCART's depletion calculations, the 4x4 array was burned up to27.5MWd/kgU (~688 effective full power days). Figure 3 shows the fuel pin layout for DeCART. As a first approximation, no guide tubes or burnable absorbers were included in the 4x4 model; however, such characteristics of PWR's will be added once initial testing of the external coupling is complete. Also, in the same figure the dotted lines separate the 25 subchannels that were modeled around the fuel pins in CTF.

General Specifications:				**Geometry:**		
Type	**Value**	**Units**		**Region**	**Value**	**Units**
Reactor	PWR			Fuel Pellet Radius	0.4905	[cm]
Layout	4 x 4			Clad Inner Radius	0.418	[cm]
Fuel Type	UO_2			Clad Outer Radius	0.475	[cm]
Enrichment	3.45	[w/o]		Pin Pitch	1.26	[cm]
Fuel Density	10.4	[g/cc]		Active Fuel Height	365.76	[cm]
Burnable Poison	None			**State Conditions:**		
Clad Type	Zircaloy-4			**Type**	**Value**	**Units**
Clad Density	6.55	[g/cc]		Array Power	1.0808	[MW]
Coolant Type	H_2O			Average Linear Heat Rate	18.5	[kW/m]
BOC Boron Loading	1000	[ppm]		Core Pressure	15.5	[Mpa]
				Mass Flow Rate	4.86	[kg/s]

Table 1 – Specifications for the 4x4 array was modeled in CTF and DeCART.

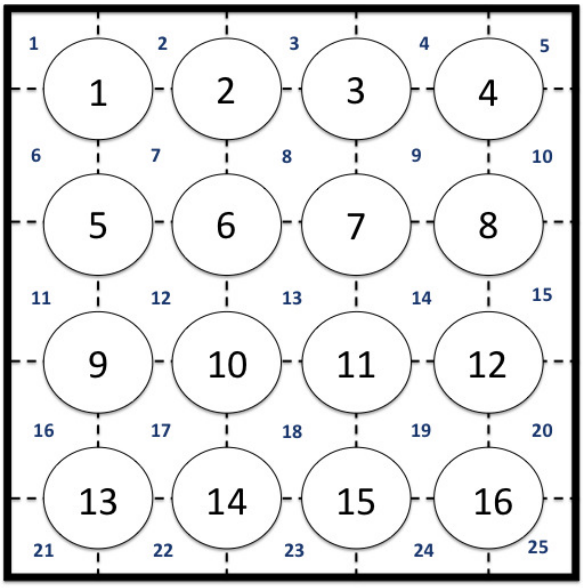

Figure 3 – 4x4 Pin Layout.

As discussed in Section 3 of the paper, inputs for DeCART and CTF were built first. The necessary parameters were exchanged between the codes, and a 10^{-3} convergence criterion was placed on the relative change between the fuel temperatures, coolant temperatures, and coolant densities in successive iterations. Convergence is measured by the relative change of some parameter from one coupled iteration to the next. For the initial testing of the offline coupling, the CTF DeCART coupled simulations converged in less than10 iterations at each depletion step. The convergence of CTF and DeCARTat beginning of cycle (BOC), i.e. 0.0 MWd/kgU, can be seen in Table 2. Only fuel temperature is shown in Table 2 because it is the parameter that took the longest to converge. Once the iterations were completed, an input model was developed for the BISON calculations. For simplicity and due to BISON's limitations, a single pin (Pin 7) was chosen from the 4x4 array to be modeled in BISON. Pin 7 was picked because it had the highest relative power compared to the other pins. The coolant (moderator) temperature profiles have been provided from CTF to BISON at different burnups. The axial power profiles have been provided from DeCART to BISON at different burnups.

Iteration	Convergence
1 (nominal)	--
2	0.114541
3	0.046258
4	0.016725
5	0.007359
6	0.003382
7	0.001825
8	0.000813

Table 2 – Fuel temperature convergence results between CTF and DeCART at BOC.

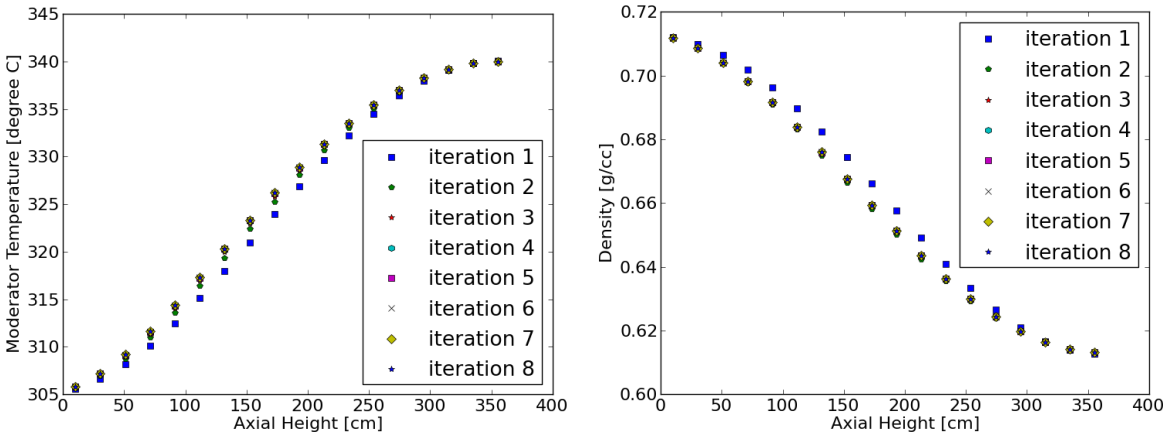

Figure 4 and 5 – Convergence of the moderator temperature and density in CTF with feedback from DeCART.

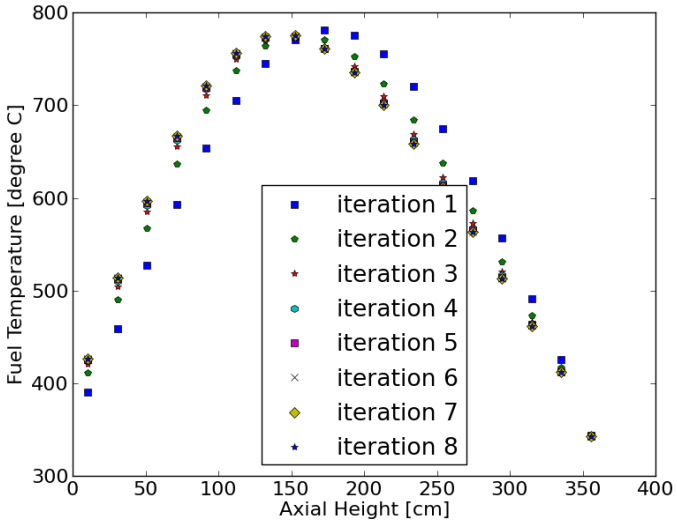

Figure 6 – Convergence of the radially averaged fuel temperature in CTF with feedback from DeCART.

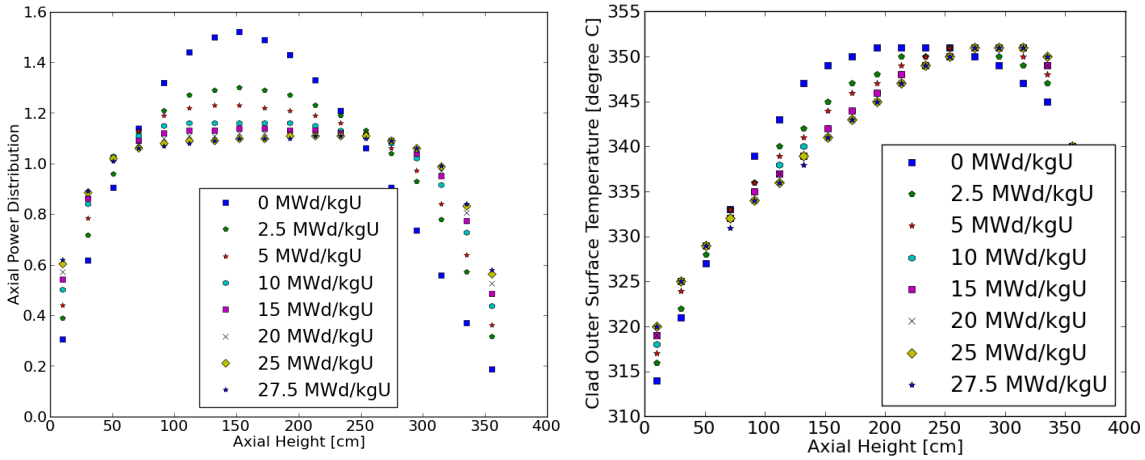

Figure 7 and 8 – Axial power and clad outer surface temperature distributions as a function of burnup.

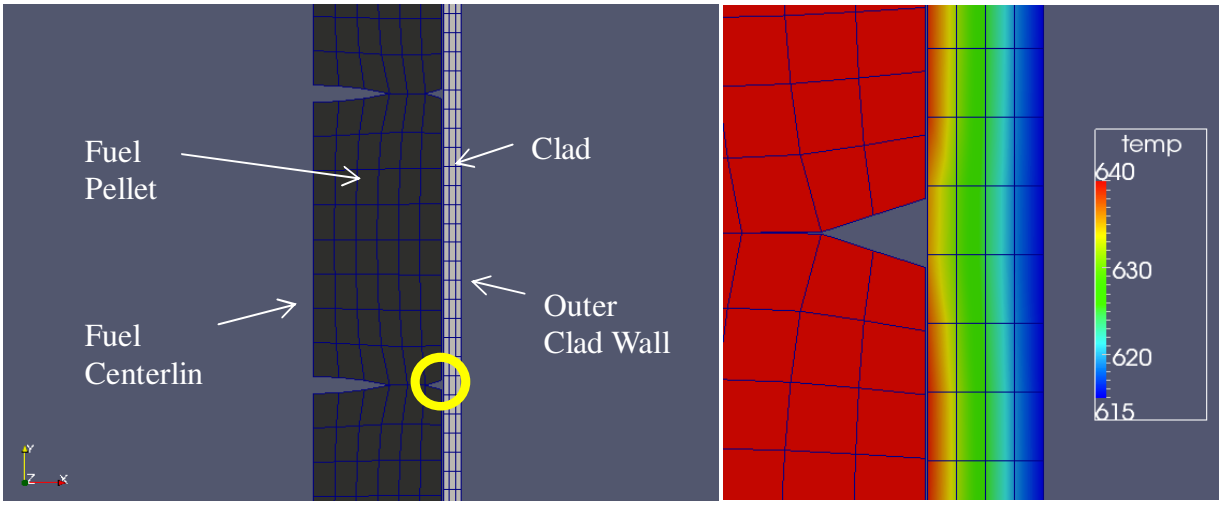

Figure 9 – (Left) Screenshot taken from the BISON mesh file that shows the fuel pellets and cladding. (Right) Screenshot taken at ~500 days into the BISON calculation with a zoomed-in view of the inter-pellet gap to show its affect on temperature.

Figures 4, 5 and 6 show the convergence of the moderator temperature, moderator density and fuel temperature, respectively at BOC (i.e. 0.0 MWD/kgU). Figure 7 shows the axial power distribution for rod 7 in the 4x4 array as a function of burnup. At each depletion step, feedback was passed between DeCART and CTF until convergence was met. During the same iteration and depletion scheme, the clad outer surface temperature profile for rod 7, shown in Figure 8, was extracted upon convergence. The power profile and temperature data from Figures 7 and 8 were used as boundary conditions for the BISON simulation. Because BISON is a finite element code, much more detail is provided in the output. The picture on the left of Figure 9 shows a detailed view of the mesh file, which contains multiple axial and radial nodes for each fuel pellet; there are 360 total fuel pellets in the full model. These capabilities allow for detailed temperature maps in the fuel and cladding, as seen in the picture on the right of Figure 9. Plots shown in Figures 10 and 11 further illustrate the detailed temperature distributions. Figure 10 shows the temperature of the cladding inner surface near the bottom of the fuel rod. The horizontal axis on the plot shows the axial locations of each node, and corresponding clad temperature. The 22 data points plotted on Figure 10 only span about 30 microns. This is a great example of how detailed BISON can be in its calculations. Figure 11 shows a similar plot to Figure 10, but further up the fuel rod at around 200 cm. Both plots were generated using the data from the last BISON time step at 27.5MWd/kgU. The calculations show that the inter-pellet region is about five degrees lower than at the pellet edge, which will engender a re-distribution of hydrogen towards the cooler region leading to a concentration of hydrides in that region. Temperature gradients such as the one shown in Figure 10 and Figure 11 will be used in the analytical model to observe its effect on hydrogen distribution in the cladding.

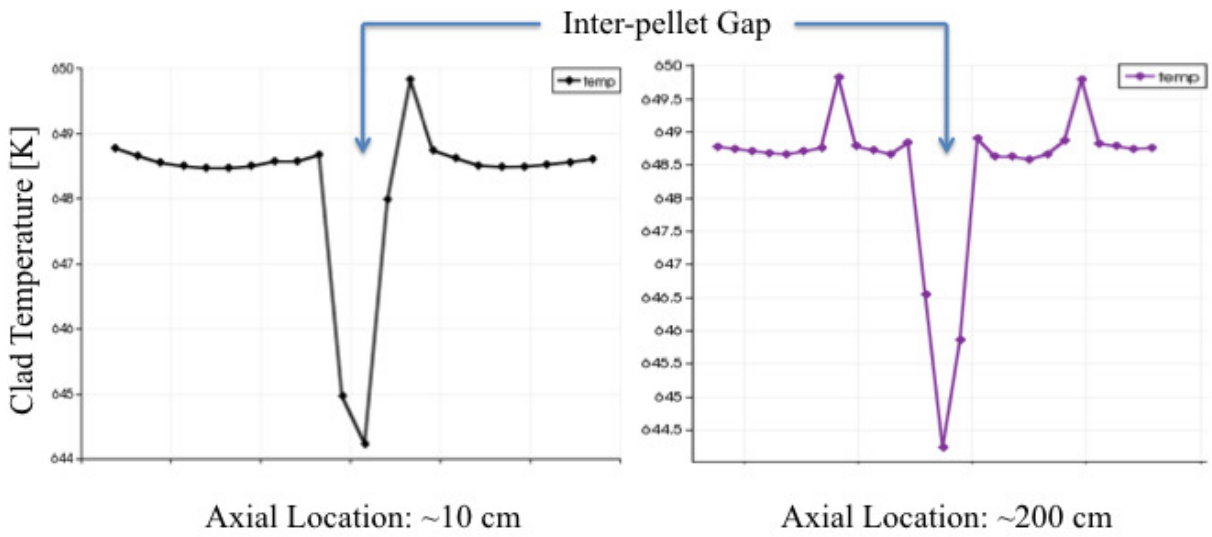

Figure 10 and 11 – Plots of the cladding inner surface temperature at different axial locations for the inter-pellet gap region shown in Figure 9.

Figure 12 shows the clad temperature in the radial direction at the inter-pellet gap. This data was taken from the last time step in BISON, and at an an axial location near the bottom of the fuel rod. Note that there is about a 35 Kelvin decrease between the inner and outer surface of the cladding.

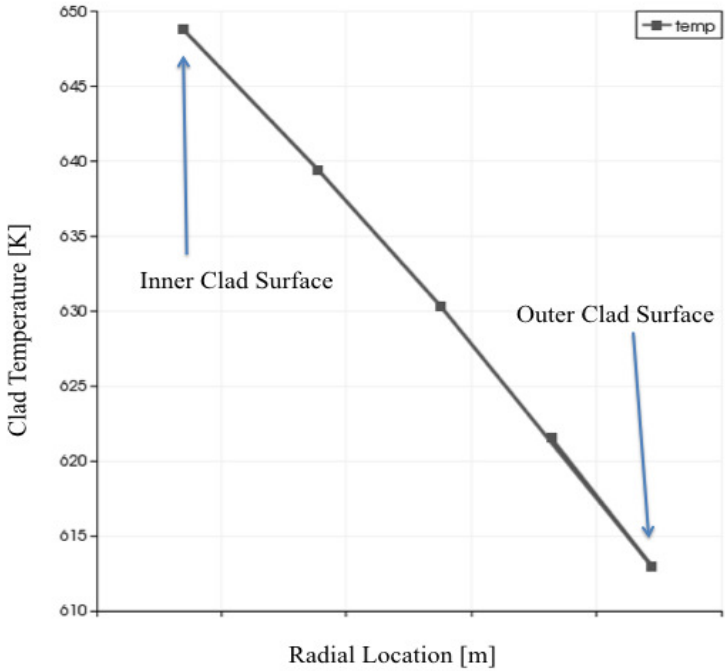

Figure 12 – Clad Temperature at the inter-pellet gap with respect to the radial direction.

5. RELATED PROJECTS

5.1 Implementation of the hydride model in BISON

In order to fulfill the hydrogen distribution prediction, according to the goals exposed in the introduction, it is necessary to implement the hydrogen model in the fuel performance code BISON. This will be done in the future and should lead to prediction of hydride distribution in an entire fuel rod.

5.2 Experimental work to improve the hydrogen distribution model

According to the hydride model, two parameters have to be determined experimentally. An experiment has been designed to calculate the heat of transport (Q*) and validate the diffusion model. The other parameter that has to be measured is the precipitation rate, which is in turn to be measured using high energy and intensity X-Ray diffraction.

5.2.1 Measurement of the heat of transport

The heat of transport can be calculated by applying a temperature gradient to a hydrided zirconium plate. After a sufficient time, the steady state equilibrium is reached and gives information about the Q* value. This experiment has been already done by Sawatzky [5] in the past. The heat of transport has also been determined by Kammenzind [10]. Our primary goal is to compare our results with the previous experiments, and to improve the accuracy of the determination of this parameter.

5.2.2 Measurement of the precipitation rate

The precipitation rate is to be measured in-situ using X-Ray diffraction. This technique allows us to measure and follow the hydride volume fraction with time[19, 20]. The experiment will measure the evolution of hydrogen concentration during a quick cooling followed by precipitation, measured by determining the area under the hydride diffraction peaks in-situ. The experiment is designed to measure the dissolution of hydride precipitates by simultaneously following the diffraction signal of the hydride phase and the shift in d-spacing from the removal of hydrogen atoms from solid solution. For this experiment, we use a homogeneous initial concentration and no specific boundary condition, in order to avoid any perturbation due to diffusion phenomena.

6. CONCLUSION

An external coupling between CTF, DeCART, and BISON was successfully completed. Initial testing of the external coupling has provided interesting results. Due to their similar meshing and structure, CTF and DeCART were able to be coupled using output information as input parameters for one another. CTF provided fuel temperatures, moderator temperatures, and moderator densities to DeCART to improve the cross-section generation. Improved cross-section generation then improves the power output calculations at depletion steps. In return, DeCART provided the pin-wise axial and radial power distributions, as well as the radial power distribution within each pin to CTF for better T-H calculations. Convergence between the two externally coupled codes provides significantly more accurate boundary conditions to be used in the BISON calculations. Single fuel pin models in BISON give detailed temperature and temperature gradient maps for both the fuel and cladding. This can be seen in Figures 10 through

12. Being able to observe relatively large temperature changes less than a millimeter apart will be important for future hydrogen/hydride distribution calculations. These cladding temperature maps are the stepping-stones to the next part of the project, implementing the analytical model for hydride distribution predictions.

7. ACKNOWLEDGMENTS

The authors would like to thank the Department of Energy (DOE) in accordance with the Nuclear Engineering University Programs (NEUP) for funding the efforts of this project (Project #: 11-2987).The authors also thank the Idaho National Laboratory for their continued support of BISON, especially Richard Williamson and Jason Hales. Furthermore, the authors thank Dan Walter from the University of Michigan for his support in the use of DeCART.

8. REFERENCES

[1] Lamarsh, J.R., Baratta, A.J., *Introduction to Nuclear Engineering*. 3rd edition 2001: Prentice Hall.

[2] Lemaignan, C. and A.T. Motta, *Zirconium Alloys in Nuclear Applications*. Materials Science and Technology. Vol. 10B. 1994: VCH.

[3] Coleman, C.E. and D. Hardie, *The hydrogen embrittlement of alpha-zirconium review.* Journal of the Less Common Metals, 1966. **11**: p. 168-185.

[4] Philippe Bossis, D.P., Karine Hanifi, Joël Thomazet, and Martine Blat, *Comparison of the High Burn-Up Corrosion on M5 and low tin Zircaloy-4.* Zirconium in the Nuclear Industry: 14th International Symposium, 2006. **STP 1467**: p. 494-524.

[5] Sawatzky, *Hydrogen in Zircaloy-2: Its distribution and heat of transport.* Journal of nuclear Materials, 1960. **4**: p. 321-328.

[6] Kearns, J.J., *Terminal solubility and partitioning of hydrogen in the alpha phase of zirconium, Zircaloy-2 and Zircaloy-4.* Journal of Nuclear Materials, 1967. **22**: p. 292-303.

[7] McMinn, A., Darby, E.C., Schofield, J.S., *The Terminal Solid Solubility of Hydrogen in Zirconium Alloys.* Zirconium in the Nuclear Industry: Twelfth International Symposium, 2000. **ASTM STP 1354**: p. 173-195.

[8] Marino, G.P., *HYDIZ: A 2-dimensonal computer program for migration of interstitial solutes of finite solubility in a thermal gradient (LWBR Development Program)*, in *AEC Research and Developement Report - WAPD-TM-1157*1974.

[9] Marino, G.P., *Hydrogen Supercharging in Zircaloy.* Materials Science and Engineering, 1971. **7**(1971): p. 335-341.

[10] Bruce F. Kammenzind, D.G.F., H. Richard Peters and Walter J. Duffin, *Hydrogen Pickup and Redistribution in Alpha-Annealed Zircaloy-4.* Zirconium in the Nuclear Industry: 11th International Symposium, 1996. **ASTM STP 1295**: p. 338-370.

[11] Avramova, M., *CTF - A Thermal-Hydraulic Subchannel Code for LWRs Transient Analyses*, K. Ivanov, Editor 2009, Penn State University: University Park, PA.

[12] Kochunas, B., Hursin, M. ,Downar, T., *DeCART-v2.05 Theory Manual*, 2009, University of Michigan.

[13] Hursin, M., Downar, T. ,Kochunas, B., *PWR Control Rod Ejection Analysis with the Method of Characteristic Code DeCART*, in *Physor*2008: Interlaken, Switzerland.

[14] Williamson, R.L., Hales, J.D., Novascone, S.R., Tonks, M.R., Gaston, D.R., Permann, C.J., Andrs, D, Martineau, R.C., *Multidimensional multiphysics simulation of nuclear behavior.* Journal of Nuclear Materials, 2012(423): p. 149-163.

[15] Williamson, R.L., Novascone, S.R., Hales, J.D., Spencer, B., *BISON Workshop*, 2012, Idaho National Laboratory: Idaho Falls, ID.

[16] Derek Gaston, J.H., *MOOSE Workshop*, 2012, Idaho National Laboratory: MIT.

[17] Hamilton, S., Clarno, K., Philip, B., Berrill, M., Sampath, R., Allu, S., *Integrated Radiation Transport and Nuclear Fuel Performance for Assembly-Level Simulations*, in *PHYSOR 2012*2012: Knoxville, TN.

[18] *SIMULATE-3: Advanced Three-Dimensional Two-Group Reactor Analysis Code*, 2009, Studsvik.

[19] Colas, K., *Fundamental experiments on hydride reorientation in Zircaloy*, in *Mechanical and Nuclear Engineering*2012, Pennsylvania State University.

[20] K. B. Colas, A.T.M., M. R. Daymond, J.D. Almer, M. Kerr, A.D. Banchik, P. Vizcaino and J.R. Santisteban, *In Situ Study of Hydride Precipitation Kinetics and Re-orientation in Zircaloy Using Synchrotron Radiation.* Acta Materiala, 2010. **58**: p. 6575-6583.